

Article

Cardiomyocyte-Specific Deletion of Orai1 Reveals Its Protective Role in Angiotensin-II-Induced Pathological Cardiac Remodeling

Sebastian Segin^{1,2}, Michael Berlin^{1,2}, Christin Richter¹, Rebekka Medert^{1,2}, Veit Flockerzi³, Paul Worley⁴, Marc Freichel^{1,2}  and Juan E. Camacho Londoño^{1,2,*} 

¹ Pharmakologisches Institut, Ruprecht-Karls-Universität Heidelberg, INF 366, 69120 Heidelberg, Germany; sebastian.segin@gmx.de (S.S.); michael.berlin@pharma.uni-heidelberg.de (M.B.); christin.richter@pharma.uni-heidelberg.de (C.R.); rebekka.medert@pharma.uni-heidelberg.de (R.M.); marc.freichel@pharma.uni-heidelberg.de (M.F.)

² DZHK (German Centre for Cardiovascular Research), Partner Site Heidelberg/Mannheim, 69120 Heidelberg, Germany

³ Experimentelle und Klinische Pharmakologie und Toxikologie, Universität des Saarlandes, 66421 Homburg, Germany; Veit.Flockerzi@uks.eu

⁴ The Solomon H. Snyder Department of Neuroscience, Johns Hopkins University, School of Medicine, Baltimore, MD 21205, USA; pworley@jhmi.edu

* Correspondence: juan.londono@pharma.uni-heidelberg.de; Tel.: +49-6221-54-86863; Fax: +49-6221-54-8644

Received: 26 March 2020; Accepted: 24 April 2020; Published: 28 April 2020



Abstract: Pathological cardiac remodeling correlates with chronic neurohumoral stimulation and abnormal Ca²⁺ signaling in cardiomyocytes. Store-operated calcium entry (SOCE) has been described in adult and neonatal murine cardiomyocytes, and Orai1 proteins act as crucial ion-conducting constituents of this calcium entry pathway that can be engaged not only by passive Ca²⁺ store depletion but also by neurohumoral stimuli such as angiotensin-II. In this study, we, therefore, analyzed the consequences of Orai1 deletion for cardiomyocyte hypertrophy in neonatal and adult cardiomyocytes as well as for other features of pathological cardiac remodeling including cardiac contractile function in vivo. Cellular hypertrophy induced by angiotensin-II in embryonic cardiomyocytes from Orai1-deficient mice was blunted in comparison to cells from litter-matched control mice. Due to lethality of mice with ubiquitous Orai1 deficiency and to selectively analyze the role of Orai1 in adult cardiomyocytes, we generated a cardiomyocyte-specific and temporally inducible Orai1 knockout mouse line (Orai1^{CM-KO}). Analysis of cardiac contractility by pressure-volume loops under basal conditions and of cardiac histology did not reveal differences between Orai1^{CM-KO} mice and controls. Moreover, deletion of Orai1 in cardiomyocytes in adult mice did not protect them from angiotensin-II-induced cardiac remodeling, but cardiomyocyte cross-sectional area and cardiac fibrosis were enhanced. These alterations in the absence of Orai1 go along with blunted angiotensin-II-induced upregulation of the expression of Myoz2 and a lack of rise in angiotensin-II-induced STIM1 and Orai3 expression. In contrast to embryonic cardiomyocytes, where Orai1 contributes to the development of cellular hypertrophy, the results obtained from deletion of Orai1 in the adult myocardium reveal a protective function of Orai1 against the development of angiotensin-II-induced cardiac remodeling, possibly involving signaling via Orai3/STIM1-calcineurin-NFAT related pathways.

Keywords: calcium; cardiac remodeling; cardiac function; Orai1 proteins; neurohumoral stimulus

1. Introduction

The main compensatory homeostatic responses to reduction of heart function are activation of the renin–angiotensin–aldosterone system (RAAS) and the sympathetic nervous system [1].

Angiotensin-II (AngII) is able to activate AT_1 -receptors which couple to $G_{q/11}$, $G_{12/13}$ - or $G_{i/o}$ and activates signaling cascades that involve the regulation of $[Ca^{2+}]_i$ and development of cardiac hypertrophy [2]. Besides its important role for contractile mechanisms, Ca^{2+} plays a fundamental function as a second messenger. It controls hypertrophic genes, e.g., via the calcineurin-NFAT-pathway by translocation of NFAT into the nucleus [3] and its homeostatic alterations underlie hallmarks (contractile dysfunction and arrhythmias) of heart failure [4]. Changes in intracellular Ca^{2+} concentration $[Ca^{2+}]_i$ and localization can be regulated by different pathways and triggers. Members of the TRPC subfamily of transient receptor potential canonical channels are involved in these processes (for review see [3,5–8]), and recently a background Ca^{2+} entry pathway (BGCE) was described in mouse adult cardiomyocytes, which is crucial for the pathological cardiac remodeling but does not modulate cardiac contractility in vivo. BGCE is significantly enhanced by AngII treatment and is mediated by TRPC1/TRPC4 channels [9]. Another crucial Ca^{2+} entry pathway into the cells, which can be evoked by receptor agonists leading to phospholipase C activation and depletion by IP_3 -sensitive Ca^{2+} stores, is the so-called store-operated Ca^{2+} entry (SOCE). This Ca^{2+} entry pathway was initially identified in non-excitabile cells and it is mediated by Ca^{2+} channels that are activated by depletion of intercellular Ca^{2+} stores to refill Ca^{2+} -depleted sarcoplasmic reticulum [10,11]. SOCE is driven by proteins of the Orai family. The Orai genes are widely expressed and encode transmembrane proteins that form highly selective Ca^{2+} channels and were first described in 2006 [12–15]. Three isoforms (Orai1, Orai2, and Orai3) are known [16,17] and Orai1 is a crucial component of SOCE in all cell types analyzed so far [18]. Ca^{2+} depletion is detected through STIM1 (Stromal Interaction Molecule 1) and STIM2 proteins, Ca^{2+} sensors located in the sarcoplasmic reticulum membrane [14,19]. STIM proteins bind Ca^{2+} as long as high sarcoplasmic reticulum Ca^{2+} concentrations are present. Following Ca^{2+} store depletion, the conformation of STIM proteins changes and the molecules oligomerize on the sarcoplasmic reticulum's surface close to the plasma membrane to activate Orai proteins through direct contact and refilling Ca^{2+} storage begins [19–22].

SOCE has been described in neonatal and adult cardiomyocytes across different species including mice and rats, as well as in cardiomyocyte cell lines [23–30]. The amplitude of SOCE in adult cells was apparently lower in comparison to neonatal cardiomyocytes cells [23], but SOCE is re-activated in adult cardiomyocytes by mechanical and neurohumoral stress including AngII treatment; concordantly, cardiac expression of Orai1 and/or Stim1 is boosted in models of cardiac hypertrophy/remodeling, such as aortic banding [23], including transverse aortic constriction (TAC) in rats [24], TAC in mice [31,32], or related stress stimuli in neonatal rat ventricular cardiomyocytes [23,25]. SOCE and Stim1-dependent signaling in the heart and its implications in its physiology and pathophysiology has been matter of review [33–36].

Deletion of Orai1 proteins leads to cardiac dysfunction with reduced systolic function, bradycardia, and skeletal myopathy in zebrafish [31] and perinatal lethality in mice that can be rescued only partially by backcrossing to an outbred mouse strain [37]. Cardiac-specific suppression of Orai1 in *Drosophila* provoked reduced contractility consistent with dilated cardiomyopathy [38]. Heterozygous Orai1^{+/-} mice of a C57BL6/J genetic background with ~25% reduction of Orai1 protein expression in the heart exhibit faster development of heart failure after TAC [39]. Initial evidence supporting the concept of a role of Orai1 in cardiac remodeling comes from the analysis of cellular models. It has been shown that Orai1 knockdown via siRNA in neonatal rat cardiomyocytes reduces SOCE and it is protective to hypertrophic stimuli such as phenylephrine [25]. Similarly, SOCE was also reduced in HL-1 cells by a similar approach [27]. More recently, the regulation of SOCE by aldosterone was proposed in neonatal rat ventricular myocytes where a dominant negative mutant of Orai1 or the Orai1 blocker S66 reduced aldosterone-induced SOCE [40]. Modulation of Orai1 through the NO (Nitric Oxide), cGMP (cyclic Guanosine Monophosphate), and protein kinase G (PKG) pathway, ending up in phosphorylation of Orai1 and reduction of SOCE, also abolished hypertrophic effects induced by phenylephrine in human embryonic stem cell-derived cardiomyocytes [41]. Orai1 expression was shown to be attenuated by gastrodin, resulting in reduced SOCE and protection from the hypertrophy-inducing

agents' phenylephrine and angiotensin-II, respectively [42]. In humans, Orai1 loss or gain of function mutations have been causally associated with myopathy and immunodeficiency [43].

To analyze the effect of complete inactivation of Orai1 for cardiac remodeling and function in the adult heart and to circumvent the potential effects of early deletion of Orai1 caused by global Orai1 deletion and mutation analysis in humans, we generated a cardiomyocyte-specific and temporally inducible Orai1 knockout mouse line. Analysis of cardiac contractility under basal conditions and after angiotensin-II infusion showed no differences between Orai1-deficient mice and control mice. Moreover, deletion of Orai1 selectively in cardiomyocytes did not evoke changes in cardiac histology and did not protect adult mice from AngII-induced cardiac remodeling. In contrast, AngII infusion resulted in increased cardiomyocyte cross-sectional area and collagen deposition, which were accompanied by differences in gene expression of Myoz2, STIM1, and Orai3 in the absence of Orai1. Thus, our results obtained from an approach with acute deletion of Ora1 in adult cardiomyocytes suggest that Orai1 proteins, unlike in embryonic cardiomyocytes, do not mediate processes of maladaptive cardiac remodeling in cardiomyocytes of adult mice in this type of cardiac pathophysiology but contribute to processes that are protective.

2. Materials and Methods

2.1. Animal Experiments

All animal experiments were approved and performed according to the regulations of the Regierungspräsidium Karlsruhe and the University of Heidelberg (AZ 35-9185.81/G131/15) and conform to the guidelines from Directive 2010/63/EU of the European Parliament on the protection of animals used for scientific purposes. Mice were maintained under specified pathogen-free conditions at the animal facility (IBF) of the Heidelberg Medical Faculty in a 12-h light-dark cycle, and water and standard food (Rod18, LASvendi GmbH, Soest, Germany) were available to consume ad libitum. Investigator and technical assistants were blinded towards genotype and treatment of the mice. Mice from single breeding pairs were randomly distributed in different treatment groups to avoid a breeding bias.

To generate Orai1^{+/-} mice (used to obtain Orai1^{-/-} embryos), we crossed Orai1^{flox/flox} mice [44] with a Cre-deleter strain [45]. To generate a cardiomyocyte-specific inducible Orai1 knock-out mouse model (Orai1^{CM-KO}), we mated Orai1^{flox/flox} mice [44] with α MHC/CreERT2 mice kindly provided by Prof. Stefan Offermanns [46]. Male Orai1^{flox/flox}/ α MHC/Cre (either Cre^{pos} or Cre^{neg}) mice were injected intraperitoneally with 1 mg of tamoxifen (T5648, Sigma-Aldrich Munich, Germany) dissolved in Miglyol (10 mg/mL) (Caelo, Hilden, Germany) for 5 consecutive days at an age of 11 weeks to induce deletion of exons 2 and 3 of the Orai1 gene. In part of the experiments, Miglyol at the same volume was given to control animals (Orai1^{flox/flox}/ α MHC/Cre^{pos} mice used as additional control for possible Cre effects independent of tamoxifen), whereas in other experiments Orai1^{flox/flox}/ α MHC/Cre^{neg} mice treated with tamoxifen were used as control. Three weeks after the last injection, animals were analyzed under nontreatment conditions or after angiotensin II (Calbiochem/Merck, Darmstadt, Germany) treatment using osmotic Mini Pumps (Alzet model 1002, DURECT Corporation, Cupertino, CA, USA) at a rate of 3mg/kg/day as previously described [9]. Mini Pumps for the control group were filled with 0.9% NaCl.

To evaluate the α MHC/Cre efficiency, we used a α MHC-mTmG reporter mouse strain and determined the efficacy of Cre-mediated recombination and tissue specificity after injection of tamoxifen or Miglyol. To generate the reporter mice, α MHC/CreERT2 mice were crossed with mice from the mTmG (*Gt(ROSA)26Sor^{tm4}(ACTB-tdTomato,-EGFP)/Luo*/J) reporter strain [47]. Tamoxifen and Miglyol treatment were done, as mentioned above.

Pressure volume loop measurements were done under isoflurane anesthesia (2% with a mixture of O₂/N₂O (1:2), Vapor 19.3, Abbot). Pancuronium (1 μ g/g body weight -BW-) and heparin (1.2 IE/g BW) were injected intraperitoneally. Mice were placed on a heating plate and temperature was monitored

to keep it at 37 °C \pm 0.6 °C. During the complete procedure, mice were intubated and ventilated (MiniVent 845, Hugo Sachs Elektronik - Harvard Apparatus GmbH, March-Hugstetten, Germany) with tidal volume = 6.2 \times body weight^{1.01}, as described [48]. Adequate depth of anesthesia was proven by the absence of the paw withdrawal reflex from the hind paws before relaxation with pancuronium. For fluid maintenance and volume calibration, a catheter (outer diameter 0.61 mm) was inserted into the femoral vein and NaCl 0.9% was constantly perfused at a rate of 10 μ L/min (11Plus, Hugo Sachs Elektronik - Harvard Apparatus GmbH, March-Hugstetten, Germany).

After thoracotomy a PVR 1035 catheter (Millar, Houston, TX, USA) connected to a MPVS Ultra (ADInstruments, Oxford, UK) was placed in the left ventricle after puncture with a 25-G needle. A suture around the inferior vena cava was used to change preload by transient occlusion of the vein for measuring the preload-independent parameters. While recording parameters with LabChart Pro 8 (ADInstruments, Oxford, UK), ventilation was stopped for a few seconds. At the end of the experiment, calibration was performed by injecting three single 10- μ L boli of hypertonic saline (15%) and taking blood for volume cuvette calibration, as described [49]. For euthanasia, the ventilation was stopped, inducing a pneumothorax and the removal of the heart produced exsanguination, both occurred under anesthesia. Organs were analyzed for water content and weight, normalized to body weight and tibia length as described [9].

2.2. Cardiomyocyte Isolation

To obtain *Orai1*^{-/-} embryonic cardiomyocytes, *Orai1*^{+/-} mice were mated and pups were taken from plug-positive females at E18.5. Hearts were isolated separately, cleaned from noncardiac tissue residues in DPBS, Mg²⁺, and Ca²⁺ free (Thermo Fisher Scientifics/Gibco, Waltham, MA, USA), digested with trypsin 0.5% (Thermo Fisher Scientifics/Life Technologies) and DNase (2.2 kU/5 mL Trypsin, Sigma), and mechanically homogenized by repeated pipetting through a blunted tip. After centrifugation (Megafuge 1.0, Heraeus, Hanau, Germany) at 319 \times g at 4 °C for 10 min, the cell pellet was resuspended in DMEM/F12 (Thermo Fisher Scientifics/Life Technologies) with 15% serum (Nu-Serum IV, BD Biosciences, San Jose, CA, USA) and seeded on cell culture plates (6-Well Cell Culture Plate, CellStar, Greiner bio-one; 10 cm² per well, Greiner, Frickenhausen, Germany). After 24 h, AngII (final concentration 100 nM in DPBS) was added to DMEM/F12 with 0.5% serum (FBS, 10270-106, Gibco) to induce cardiomyocyte hypertrophy. The control group received only DMEM/F12 with 0.5% serum. Cellular hypertrophy was compared in terms of change in cell area normalized to the mean value of the corresponding control condition.

Adult cardiomyocytes were isolated as previously described [9]. First, hearts were washed with oxygenated 200 μ M EGTA containing perfusion buffer (134 mM NaCl, 11 mM Glucose, 4 mM KCl, 1.2 mM MgSO₄, 1.2 mM Na₂HPO₄, 10 mM HEPES, pH 7.35) for 3 min. Then, hearts were perfused with oxygenated digestion buffer (perfusion buffer with 0.05 mg/mL Liberase TM, Roche Applied Science, Pleasanton, CA, USA) for 2–3 min. Atria were then separated from the ventricle and ventricular cells were dissociated by gentle pipetting. Tissue rests were removed by filtration through a 100- μ m filter (Sysmex, Norderstedt, Germany) and extracellular Ca²⁺ concentration was stepwise increased to 1 mM. For expression analysis of enriched cardiomyocyte preparations, cells were purified by one decantation step (10 min/RT 22–24 °C) and two consecutive centrifugation steps (1 \times 47 \times g 1.5 min and 1 \times 47 \times g 1 min). Finally, PBS-washed pellets were resuspended in 500- μ L TRIzol reagent (Thermo Fisher Scientifics/Invitrogen), frozen in dry ice, and stored at –80 °C until RNA isolation. For microscopy, cardiomyocytes were seeded on Extra Cellular Matrix-coated coverslips (ECM Gel from Engelbreth-Holm-Swarm murine sarcoma, E1270, Sigma). Afterwards, fixation was done with paraformaldehyde (PFA 4% in PBS pH 7.4, 10 min at 4 °C), until analysis cells were stored at 4 °C in PBS containing 0.2% Na-Azide.

Fluorescence images were obtained with an inverted microscope Z1 (Zeiss, Jena, Germany) equipped with a Digital Camera AxioCamMRm (Zeiss), a DG4 Plus/30 Lamp (Sutter Instrument Company, Novato, CA, USA), and appropriate DIC, 45-Texas Red and YFP filters (AHF analysentechnik

AG, Tübingen, Germany), and control Software (AxioVision 4.8, multichannel module, Zeiss). For the analysis of adult cardiomyocytes from reporter mice (α MHC-mT/mG), images were taken with a Fluar objective (20 \times /0.75DICII (DIC.5-1.4), Zeiss) and the exposure times were 15–35 ms for bright field, 700 ms for red fluorescence, and 250 ms for the green fluorescence).

2.3. Analysis of *Orai1* Expression and Cellular Hypertrophy by Immunocytochemistry

After fixation, cells were placed into $-20\text{ }^{\circ}\text{C}$ acetone for 5 min for permeabilization, then rinsed with chilled PBS and incubated at room temperature with 1% BSA (Carl Roth, GmbH, Karlsruhe, Germany) in PBST (PBS + 0.1% *v/v* Tween-20 and including 0.3 M Glycine). Cells were incubated over night with the primary antibody (anti- α -Actinin 1:800 (ACTN2) clone EA-53, Sigma) for cell size analysis and identification of cardiomyocytes or anti-*Orai1* (#1003, 1:200) to detect *Orai1* proteins [50] at $4\text{ }^{\circ}\text{C}$. Afterwards, cells were washed three times with chilled PBS. Incubation with the secondary antibody (1:200 either anti-rabbit AlexaFluor488 or anti-mouse AlexaFluor594, Thermo Fisher Scientific/Invitrogen) was done for 2 h for anti-*Orai1* and for 1 h for all other antibodies. Nuclei were stained using DAPI (4',6-diamidino-2-phenylindole, Thermo Fisher Scientific/Invitrogen) (1.5 $\mu\text{g}/\text{mL}$ in PBS for 5 min). During incubation times, the cells were protected from light to avoid fading. Afterwards, cells were mounted and covered in anti-fade (6 g Glycerin, 2.4 g Mowiol 4–88, 6 mL ddH₂O, 12 mL Tris-HCl 0.2 M pH 8.5, and DABCO 25 mg/mL solution). Cell size was analyzed after staining using the α -Actinin antibody under a fluorescence microscope (Z1, Zeiss) using the quantification tool of the AxioVision software 4.8 (Zeiss).

2.4. RNA Isolation and qPCR Analysis

RNA isolation from Langendorff heart-derived cell populations or heart samples was performed using the TRIzol reagent (Thermo Fisher Scientific/Invitrogen) including two final ethanol washing steps before RNA resuspension. When required, isolated RNA was further purified by 3–5 additional extraction steps with one volume of diethyl ether and a final ethanol precipitation with 0.3 M potassium acetate. DNA digestion was performed with the Turbo DNA-freeTM kit (Thermo Fisher Scientific/ambion) following the instructions of the manufacturer with two DNase incubation steps. Purity, integrity, and quantity of the RNA samples were controlled by spectrophotometry (NanoQuant, Tecan, Männedorf, Switzerland), microfluidic analysis (BioAnalyzer 2100, Agilent Technologies, Santa Clara, CA, USA), and fluorometry (qbit assay, ThermoFisher Scientific), respectively. RNA was separated in several aliquots and stored at $-80\text{ }^{\circ}\text{C}$ in order to use only freshly thawed RNA for qPCR experiments. Then, cDNA synthesis from 1000 ng of RNA was carried out using a SuperScript first-strand synthesis system for RT-PCR (SensiFAST BIO-65054, BIOLINE, London, UK). Fifty ng cDNA from each sample were used as template. In brief, qPCR was performed with a Universal Probe Library (Roche) (probes and primers listed in Table S3) by using Roche FastStart Essential DNA Probes MasterMix (Roche 06402682001) and detection on a Light Cycler96 (Roche). Thermal cycling conditions included: Initial denaturing at $95\text{ }^{\circ}\text{C}$ for 600 s, followed by 40 cycles of amplification (each cycle: 10 s/ $95\text{ }^{\circ}\text{C}$, 30 s/ $60\text{ }^{\circ}\text{C}$). The standard curve quantization method was used for gene expression measurements. Values are expressed as relative expression and calculated as follows:

$$\text{Relative Expression} = (\text{Mean } E^{-Cq} / \text{Mean } E_{\text{HKG}}^{-Cq}) / ((\text{Mean } E_{\text{HKG}} / 100 + 1)^{-Cq} \times 10^4) \quad (1)$$

with E being the efficiency, Cq the cycle of quantification, and HKG refers to housekeeping genes.

All PCR reactions were performed in duplicate and normalized to the expression of the housekeeping genes H3F3A, AIP, and CXXC1, as done before [51]. In case of heart samples, only the H3F3A and CXXC1 genes were used for normalization since AngII treatment produced a significant upregulation of the AIP gene in control mice.

2.5. Histological Analysis

Briefly, and as described before [9], cardiac tissue was fixed for 24 h with 4% paraformaldehyde in PBS (pH 7.4). Processing of the tissue was done in a Tissue Processor (Leica TP 1020, Leica Biosystems, Wetzlar, Germany) over 24 h and samples were manually embedded in paraffin. For cross-sectional area analysis and cardiac fibrosis, heart sections were stained with hematoxylin eosin (HE) or Sirius red (SR), respectively. Images were taken and analyzed with AxioVision 4.8 (Zeiss).

2.6. Statistical Analysis

Data were analyzed with Excel 2011 (Microsoft, Redmond, WA, USA) and Origin 8 (OriginLab Corporation, Northampton, MA, USA). Values are shown as mean \pm standard deviation. Statistical significances were assumed when $p < 0.05$. The p values are depicted as * $p < 0.05$, ** $p < 0.01$, and *** $p < 0.001$. Statistical analysis was performed using the appropriate tests (unpaired Student's t -test, two-way ANOVA, Kruskal–Wallis) after normality test (Shapiro–Wilk normality test). Two-way ANOVA tests were followed by Bonferroni's post hoc comparisons to test specific pair comparisons and Dunn's test after Kruskal–Wallis.

3. Results

3.1. *Orai1* Deletion Protects from Neurohumorally Induced Cellular Hypertrophy in Embryonic Cardiomyocytes

Since global *Orai1* deletion leads to perinatal lethality in mice [37,52], we utilized prenatal cardiomyocytes (E18.5) for the evaluation of the role of *Orai1* in the development of cellular hypertrophy in vitro. We intercrossed *Orai1*^{+/-} mice to obtain *Orai1*^{-/-}, *Orai1*^{+/-}, and *Orai1*^{+/+} cardiomyocytes. After immunocytochemical analysis of cells stained with anti-*Orai1* antibody, we detected expression of *Orai1* proteins in cells from wild-type (WT) mice. Specificity of the immunostaining was demonstrated in cells from *Orai1*^{-/-} embryos. *Orai1* expression was also detected in *Orai1*^{+/-} cells (Figure 1A). Here, cardiomyocytes were identifiable through staining for α -Actinin, confirming the expression of *Orai1* in cardiomyocytes and in α -Actinin-negative cardiac cells at this developmental stage. In cells isolated from *Orai1*^{-/-} embryos, the hypertrophic stimulation using angiotensin-II (AngII) did not result in an increase of cardiomyocyte area, in contrast to *Orai1*^{+/+} and *Orai1*^{+/-} cells, which both showed a significant rise in cell size (Figure 1B). In our hands, angiotensin-II alone was effective in inducing hypertrophic effects in cardiomyocytes in WT cells and produced a stronger effect ($p < 0.001$) than phenylephrine after 72 h (Figure S1).

3.2. Unaltered Cardiac Function in Cardiomyocyte-Specific *Orai1*-Deficient Mice

Firstly, we analyzed the efficiency of the Cre recombinase expressed under the cardiomyocyte specific promoter α MHC assessing Cre-dependent GFP fluorescence in isolated adult cardiac myocytes and we found GFP expression only in mTmG/ α MHC-Cre^{POS} mice (Figure S2) with 99.7% of the cardiomyocytes being GFP-positive; notably, no GFP-positive cells were observed in the control group. At the tissue level Cre activity was observed only in cardiac tissue and in a restricted portion of large-diameter blood vessels of the lungs (Figure S2). All together, these results indicate a highly efficient and restricted expression pattern of the α MHC-Cre transgene used here for *Orai1* deletion in cardiomyocytes. To further analyze the role of *Orai1* in adult cardiomyocytes, we only used a tamoxifen-Cre-based inducible model for specific deletion of *Orai1* in adult mice (referred always as *Orai1*^{CM-KO}). With this model, we pursued to circumvent the lethality during early developmental stages or possible developmental effects if *Orai1* is constitutively deleted in the heart in early stages. In isolated adult cardiomyocytes from *Orai1*^{CM-KO} (*Orai1*^{flox/flox}/ α MHC/Cre^{POS}) mice we observed a reduction by $81.4 \pm 5.4\%$ in *Orai1* transcript levels compared to controls (*Orai1*^{flox/flox}/ α MHC/Cre^{neg}) (Figure 2A). We performed immunocytochemistry stainings in cardiomyocytes from adult WT and *Orai1*^{CM-KO} mice using different anti-*Orai1* antibodies. However, we were not able to specifically

observe its expression in these adult cells by this method (data not shown). The remaining Orai1 transcripts were likely to stem from noncardiomyocyte cells, as it is known that one cannot entirely get rid of nonmyocytes by this isolation procedure. In addition, we analyzed the expression of other genes important in intracellular Ca^{2+} signaling, and observed in Orai1^{CM-KO} cardiomyocytes a significant downregulation of Orai3 (by $17 \pm 4.3\%$), Stim2 (by $30.2 \pm 6.6\%$), and Saraf (by $16.5 \pm 6.5\%$) expression (Figure 2A). In contrast, no significant changes were observed in the expression of Orai2, Stim1, Trpc1, Trpc3, Trpc4, and Trpc6 (Figure 2A). We then analyzed whether Orai1 deletion in cardiomyocytes provoked any allometric change. The allometric analysis (Table S1) showed that Orai1^{CM-KO} mice were lighter (control 30.22 g vs. Orai1^{CM-KO} 27.72 g, $p = 0.046$) and showed lighter livers (1461 mg vs. 1251 mg, $p = 0.011$) and increased liver water content (66.8% vs. 67.9%, $p = 0.015$). The heart weight was comparable between both groups (133 mg vs. 129 mg, $p = 0.481$), also in relation to the tibia length (Figure 2B). Here, the reduction of the heart weight to body weight ratio is explained by the reduction in body weight of Orai1^{CM-KO} mice. Analysis of cardiomyocyte cross-sectional area and cardiac fibrosis were not different between both genotypes (Figure 2C). In addition, all parameters of cardiac contractile function including cardiac output, preload recruitable stroke work (PRSW), and ejection fraction, as well as volumetric parameters, such as end-diastolic pressure volume relationship (EDPVR), were unaltered in Orai1^{CM-KO} mice (Figure 2D) compared to control animals. Also, other systolic and diastolic (e.g., Tau) parameters obtained from PV loop measurements remained unaffected by Orai1 deletion in cardiomyocytes (Table 1).

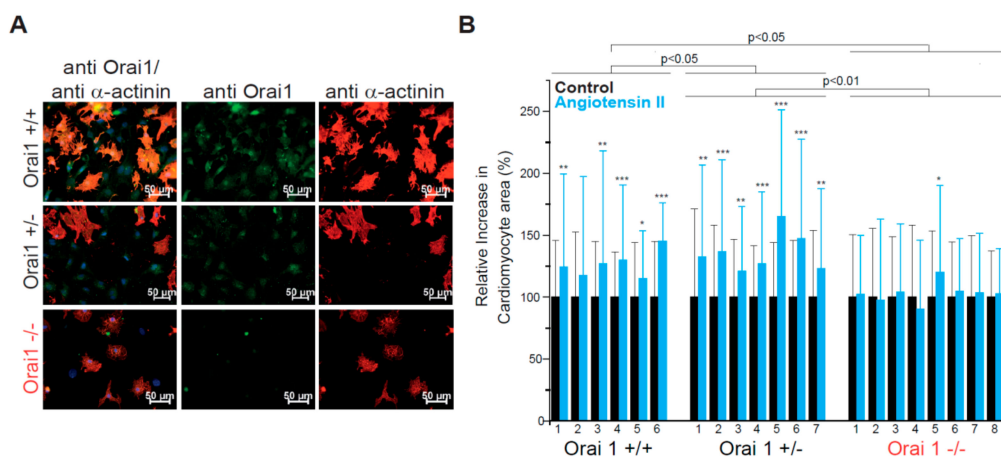


Figure 1. Orai1 is expressed in embryonic murine cardiomyocytes and its genetic deletion protects from neurohumoral-induced cellular hypertrophy. **(A)** Detection of Orai1 proteins (green) by immunocytochemistry in embryonic cardiomyocytes. As control for antibody specificity, cardiomyocytes from global Orai1-deficient (Orai1^{-/-}) mice were used. Staining with α -Actinin (red) was used to identify cardiomyocytes and DAPI (blue) to stain the nuclei. **(B)** Relative increase of cardiomyocyte area after angiotensin-II stimulation (100 nM, 72 h). Orai1^{+/+} (n = 6 hearts) and Orai1^{+/-} (n = 7 hearts) cardiomyocytes showed a significant increase in cell size while Orai1^{-/-} (n = 8 hearts) cells remained at a similar size. Number under bars indicates individual animals; * $p < 0.05$, ** $p < 0.01$, *** $p < 0.001$ for comparison between control and treatment from each isolation/heart and depicted p-values comparing between genotypes were obtained after Kruskal–Wallis and Dunn’s comparisons.

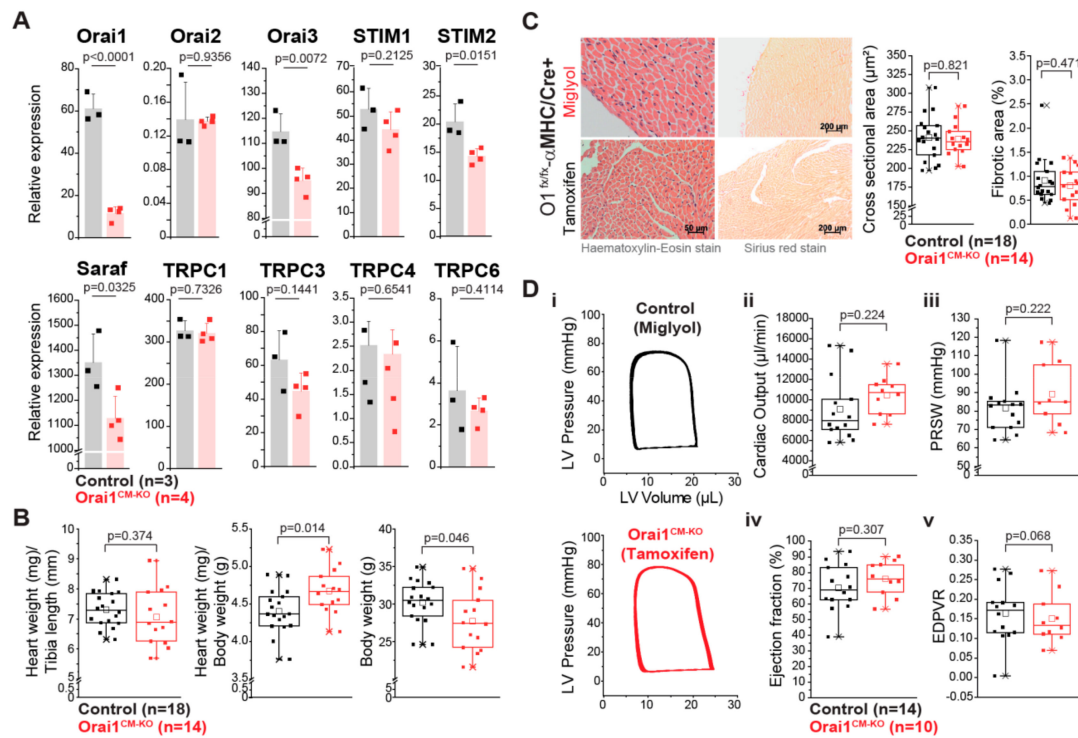


Figure 2. Mice with cardiomyocyte-specific deletion of Orai1 exhibit normal cardiac function. (A) Expression analysis of Orai1, Orai2, Orai3, STIM1, STIM2, SARAF, and TRPCs transcripts from enriched adult cardiomyocyte preparations of Orai1^{CM-KO} mice (Orai1^{flx/flx}/αMHC-Cre^{pos} + tamoxifen) by qPCR and compared to preparations from control mice (Orai1^{flx/flx}/αMHC-Cre^{pos} + Miglyol). (B) Analysis of basal cardiac hypertrophy indexes and body weight in Orai1^{flx/flx}/αMHC-Cre^{pos} mice receiving Miglyol (Control) or tamoxifen (Orai1^{CM-KO}). (C) Analysis of cardiomyocyte cross-sectional area and ventricular fibrosis from mice shown in (B). (D) In vivo cardiac function in Orai1-deficient mice (Orai1^{flx/flx}/αMHC-Cre^{pos} + tamoxifen) analyzed by PV loop analysis and compared to control mice (Orai1^{flx/flx}/αMHC-Cre^{pos} + Miglyol). Ejection fraction, cardiac output, preload recruitable stroke work (PRSW), and end-diastolic pressure volume relationship (EDPVR), are shown; n = number of mice, and p values are depicted according to the Student’s t-test.

Table 1. Pressure-volume analysis in Orai1-WT and Orai1^{CM-KO} mice. Here Orai1^{flx/flx}/αMHC/Cre^{Pos} mice treated either with Miglyol (Orai1-WT) or with tamoxifen (Orai1^{CM-KO}) were compared.

	Orai1-WT	Orai1 ^{CM-KO}	p-Value
	n = 14	n = 10	
Body temperature (°C)	37.19 (±0.56)	37.34 (±0.71)	0.534
HR (bpm)	597.2 (±35.5)	603.1 (±27.0)	0.665
ESP (mmHg)	67.3 (±6.4)	64.4 (±7.7)	0.324
EDP (mmHg)	8.4 (±3.0)	7.4 (±3.3)	0.451
ESV (μL)	8.1 (±5.7)	6.8 (±4.0)	0.530
EDV (μL)	21.8 (±7.8)	22.9 (±5.3)	0.702
SV (μL)	15.1 (±4.8)	17.3 (±2.8)	0.216
CO (μL/min)	9071.6 (±3101.2)	10442.5 (±1798.1)	0.224
Systolic parameters			
EF (%)	71.3 (±16.7)	76.1 (±11.2)	0.442
Stroke Work (mmHg x μL)	883.5 (±317.1)	962.1 (±162.3)	0.482
dP/dt max. (mmHg/s)	6591.9 (±1143.2)	6492.4 (±690.8)	0.809
PRSW	81.4 (±13.2)	89.3 (±16.7)	0.222
ESPVR	17.8 (±18.9)	12.7 (±4.5)	0.534

Table 1. Cont.

	Orai1-WT	Orai1 ^{CM-KO}	p-Value
Diastolic parameters			
Tau (ms)	7.0 (±2.6)	6.3 (±1.1)	0.407
EDPVR	0.16 (±0.07)	0.15 (±0.06)	0.677
dP/dt min. (mmHg/s)	−6679.5 (±1295.3)	−6522.3 (±622.8)	0.727

The n = number of mice, HR: Heart rate, ESP: End-systolic pressure, EDP: End-diastolic pressure, ESV: End-systolic volume, EDV: End-diastolic volume, SV: Stroke volume, CO: Cardiac output, EF: Ejection fraction, dP/dt max.: Maximum pressure increase, PRSW: Preload recruitable stroke work, ESPVR: End-systolic pressure-volume-relation, EDPVR: End-diastolic pressure-volume-relation, dP/dt min.: Minimal pressure increase. Values are given as mean ± SD.

3.3. Deletion of Orai1 in Cardiomyocytes Aggravates the Outcome of Morphometric and Functional Parameters after Angiotensin-II-Induced Cardiac Remodeling

After two weeks of systemic administration of AngII to Orai1^{CM-KO} mice an allometric analysis was performed (Table S2). A significant increase in heart weight (136.31 mg in control/NaCl vs. 173.7 mg in control/AngII $p < 0.001$, 140.69 mg in Orai1^{CM-KO}/NaCl vs. 186.66 mg in Orai1^{CM-KO}/AngII, $p < 0.001$) accompanied by significant reduction in body weight was observed in both genotypes after AngII treatment. The hypertrophy indices heart weight/body weight and heart weight/tibia length were similarly increased by AngII in both genotypes (Figure 3A). In contrast, histological analysis of cardiac sections revealed that chronic AngII treatment leads to an increase in cardiomyocyte cross-sectional area and in fibrosis (2-way ANOVA, $p < 0.0001$), and that AngII-evoked cardiomyocyte hypertrophy (Figure 3B) and fibrosis (Figure 3C) were aggravated upon Orai1 deletion in cardiomyocytes. Beyond that, liver weight was reduced significantly by the AngII treatment (2-way ANOVA, $p = 0.0003$) independent of the genotype ($p = 0.0597$, 1572.03 mg in control/NaCl vs. 1303.15mg in control/AngII $p < 0.01$, 1406.77 mg in Orai1^{CM-KO}/NaCl vs. 1262.26 mg in Orai1^{CM-KO}/AngII, $p = 0.308$), even though the water content was increased (66.35% vs. 69.09% $p < 0.001$, 66.80% vs. 68.94% $p < 0.001$). Expression analysis of hypertrophy markers showed that β MHC mRNA levels were significantly higher in hearts from Orai1^{CM-KO} mice at the end of AngII treatment compared to control mice (Figure 3D). Other hypertrophy markers such as ANP, BNP, and the skeletal- α -actin were similarly increased in both genotypes (Figure 3D). The fibrosis markers including TGF- β 2, TGF- β 3, CTGF, Collagen -I and Collagen-III were similarly increased after AngII in both genotypes (Figure 3E).

Analysis of parameters of cardiac contractility revealed that AngII treatment did not evoke changes in EF, cardiac output, and PRSW in the control group (Figure 4B,C). However, the ejection fraction in Orai1^{CM-KO} mice was reduced independently of the treatment (2-way ANOVA, $p = 0.0010$), but cardiac output, PRSW, and EDPVR were not significantly altered between genotypes. Remarkably, after AngII treatment, the end-diastolic volume was decreased in Orai1^{CM-KO} mice (21.85 μ L vs. 16.11 μ L $p = 0.025$) but not in controls (18.15 μ L vs. 15.63 μ L $p = 0.319$) as well as the stroke volume (16.16 μ L in Orai1^{CM-KO}/NaCl vs. 11.41 μ L in Orai1^{CM-KO}/AngII $p = 0.025$), which also remained unchanged upon AngII treatment in control mice (13.46 μ L vs. 13.57 μ L, $p = 0.631$) (Table 2). Finally, diastolic parameters (Tau, EDPVR) were unaffected by both AngII treatment and Orai1 deletion (Figure 4C and Table 2).

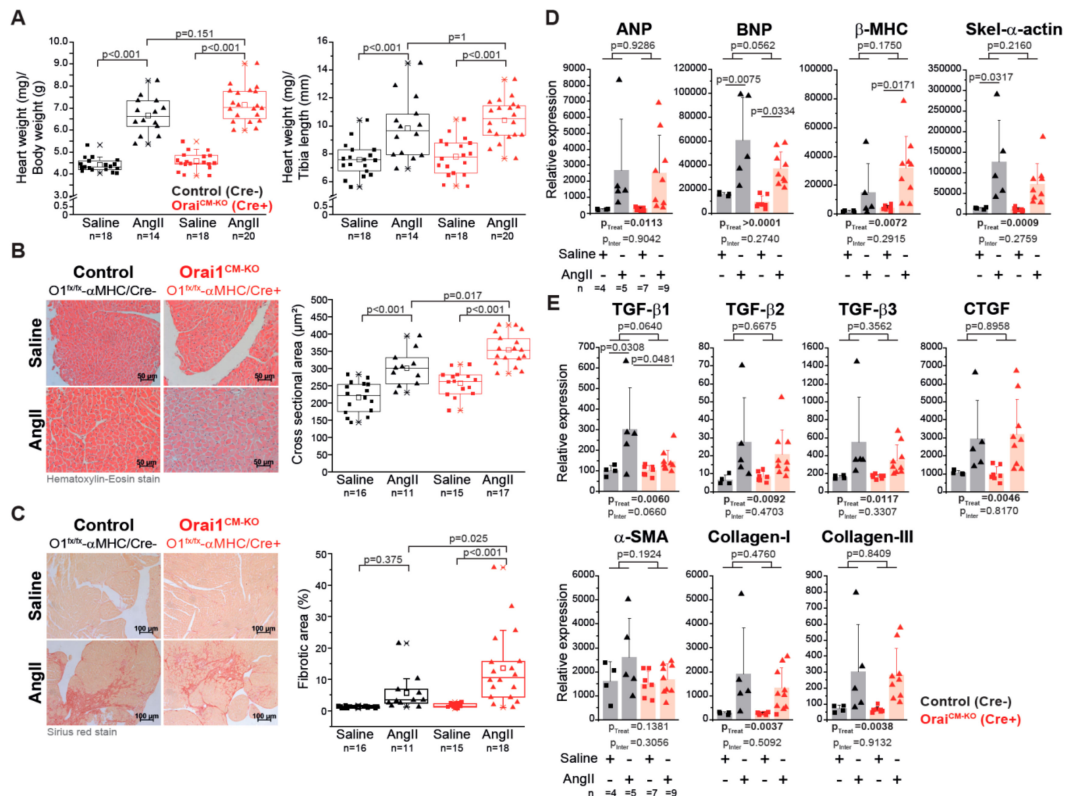


Figure 3. Cardiomyocyte-specific deletion of Orai1 aggravates angiotensin-II-induced cardiac remodeling. (A) Analysis of cardiac hypertrophy indexes in Orai1-deficient mice (red, Orai1^{lox/lox}/αMHC-Cre^{pos} + tamoxifen) and control mice (black, Orai1^{lox/lox}/αMHC-Cre^{neg} + tamoxifen) after angiotensin-II (AngII) treatment. (B) The effect of AngII on cardiomyocyte cross-sectional area in Orai1^{CM-KO} mice was analyzed. (C) Analysis of the AngII-induced ventricular fibrosis between control and Orai1^{CM-KO} mice is shown. Expression analysis (qPCR) of genes associated with the development of cardiac hypertrophy (D) and interstitial fibrosis (E) in control (black, Orai1^{lox/lox}/αMHC-Cre^{neg} + tamoxifen) and Orai1^{CM-KO} (red, Orai1^{lox/lox}/αMHC-Cre^{pos} + tamoxifen) mice after AngII treatment. The n = number of mice, and p-values are depicted according to Bonferroni's post hoc comparisons after 2-way ANOVA; p_{treat}: p-value related to the effect of AngII; p_{inter}: p-value of the interaction between AngII and genotype from 2-Way ANOVA analysis.

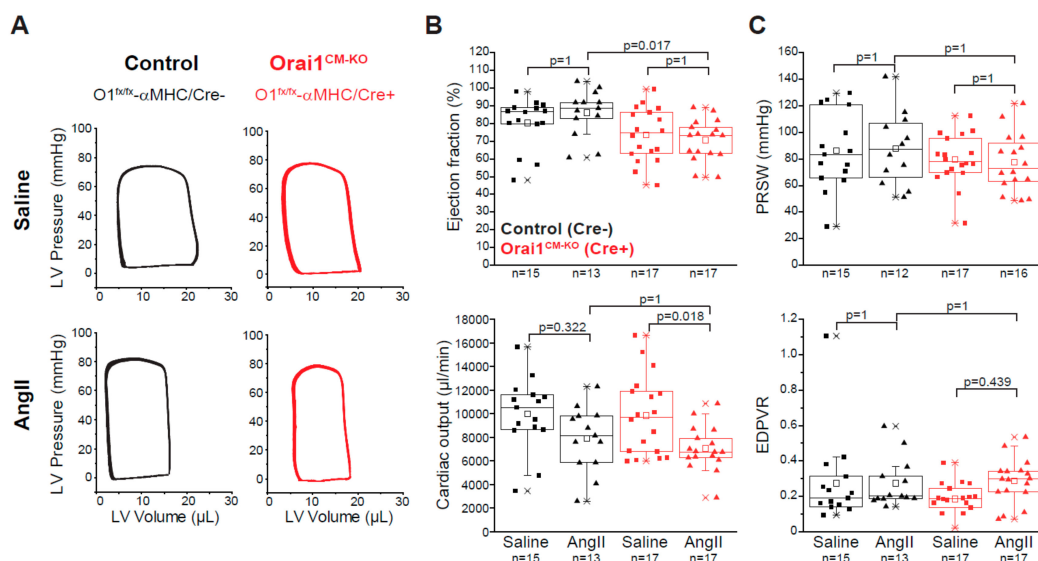


Figure 4. Cardiac function in Orai1^{CM-KO} mice after chronic angiotensin-II treatment. (A) Representative pressure-volume loops from saline- and AngII-treated control (black, Orai1^{lox/lox}/αMHC-Cre^{neg} + tamoxifen)

and *Orai1*^{CM-KO} (red, *Orai1*^{flox/flox}/ α MHC-Cre^{Pos} + tamoxifen) mice. (B–C) Analysis of cardiac contractility showing ejection fraction, cardiac output, preload recruitable stroke work (PRSW), and end-diastolic pressure volume relationship (EDPVR). The n = number of mice, and p values are depicted according to Bonferroni's post hoc comparisons after 2-way ANOVA.

3.4. Differential Gene Expression in *Orai1*^{CM-KO} Hearts after Neurohumorally Induced Cardiac Remodelling

Finally, we analyzed if *Orai1* deletion in cardiomyocytes affects the expression of (1) genes encoding proteins with known impact on SOCE activity, (2) genes encoding TRPC channels that might functionally interact with *Orai1* channels [53], and (3) genes that may be activated downstream of *Orai1* as Ca²⁺-dependent signaling molecules determining pathological cardiac remodeling. AngII treatment produced a significantly increased expression of *Orai1* and *Stim1* in control but not in *Orai1*^{CM-KO} hearts (Figure 5A), indicating a relatively restricted regulation of these genes to cardiomyocytes under AngII treatment and control of *Stim1* expression by *Orai1*. In contrast, *Orai2* expression was similarly increased by AngII in both groups, whereas *Stim2* and *Saraf* expression were unaffected by AngII treatment (Figure 5A). Like *Stim1*, *Trpc4*, and *Trpc6* expression increased in control mice treated with AngII but not in *Orai1*^{CM-KO} mice. Expression of *Trpc1* and *Trpc3* was unaffected by both genotype and AngII treatment (Figure 5B). Remarkably, we observed that the increased expression of the negative regulator of calcineurin, *Myoz2* (*Calsarcin-1*), in AngII-treated control mice was completely absent in *Orai1*^{CM-KO} mice; additionally, the effect of AngII observed in controls hearts on *Rcan1*, another calcineurin regulator, was significantly reduced in *Orai1*^{CM-KO} hearts without changes in the calcineurin A alpha expression (*Ppp3ca*) (Figure 5C). In contrast, similar effects between control and *Orai1*^{CM-KO} mice were observed after AngII-induced cardiac remodeling in regards to *Mef2a* downregulation and increased expression of one of its targets, *Myomaxin*, (Figure 5C), suggesting no obvious involvement of *Orai1* on MEF2a-dependent transcriptional activity.

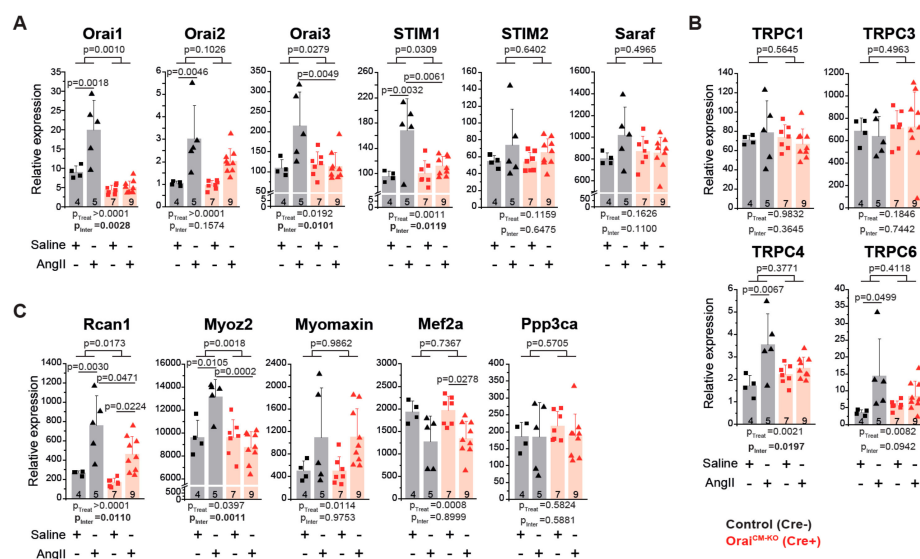


Figure 5. Analysis of *Orai1*-associated transcriptional regulation in neurohumoral-induced cardiac remodeling. Expression analysis (qPCR) in cardiac samples from control (black, *Orai1*^{flox/flox}/ α MHC/Cre^{Neg} + tamoxifen) and *Orai1*^{CM-KO} (red, *Orai1*^{flox/flox}/ α MHC/Cre^{Pos} + tamoxifen) mice via qPCR after AngII treatment. (A) Quantitative analysis of *Orai1* genes and other genes critical for the store-operated calcium entry. (B) Analysis of cation channels from the TRPC subfamily. (C) Analysis of genes associated with Ca²⁺-mediated signaling during cardiac remodeling. *Rcan1*: Endogenous calcineurin reporter, *Myoz2* (*Calsarcin-1*): Negative modulator of calcineurin, *Myomaxin*: Transcriptional target of MEF2a, *Mef2a*: DNA-binding transcription factor that activates muscle-specific, growth factor-induced, and stress-induced genes, and *Ppp3ca* (*Calcineurin A alpha*): Cardiac hypertrophy regulator through transcription factors like NFAT. The n = number of mice, and p-values are depicted according to Bonferroni's post hoc comparisons after 2-way ANOVA.

Table 2. Pressure-volume analysis after angiotensin-II treatment in Orai1-WT and Orai1^{CM-KO} mice. Here Orai1^{flox/flox/αMHC/Cre^{Neg}} (Orai1-WT) or Orai1^{flox/flox/αMHC/Cre^{Pos}} (Orai1^{CM-KO}) mice, both groups treated with tamoxifen, were compared.

	Orai1-WT		p-1	Orai1 ^{CM-KO}		p-2	p-3
	NaCl 0.9% n = 15	AngII n = 13/12		NaCl 0.9% n = 17	AngII n = 17/16		
Body temp.(°C)	36.57 (±0.45)	36.95 (±0.77)	0.803	36.76 (±0.86)	37.12 (±0.52)	0.701	1
HF (bpm)	607.42 (±31.99)	583.5 (±37.78)	0.323	620.58 (±29.65)	614.93 (±29.33)	1	0.060
ESP (mmHg)	63.71 (±9.20)	63.19 (±13.57)	1	64.40 (±10.75)	66.33 (±10.52)	1	1
EDP (mmHg)	6.53 (±3.49)	3.14 (±2.99)	0.052	3.87 (±2.99)	3.11 (±3.61)	1	1
ESV (μL)	4.43 (±2.77)	2.87 (±2.35)	1	6.97 (±4.18)	5.79 (±4.04)	1	0.164
EDV (μL)	19.83 (±5.61)	15.63 (±4.97)	0.319	21.85 (±6.24)	16.11 (±5.42)	0.025	1
SV (μL)	16.46 (±5.16)	13.57 (±4.84)	0.361	16.16 (±5.35)	11.41 (±2.88)	0.021	0.589
CO (μL/min)	9989.75 (±3052.44)	7897.54 (±2726.28)	0.211	10024.73 (±3361.74)	7044.08 (±1856.75)	0.015	0.8417
Systolic parameters							
EF (%)	80.36 (±14.30)	86.02 (±13.32)	1	72.10 (±14.01)	70.69 (±11.55)	1	0.016
Stroke Work (mmHg x μL)	990.61 (±334.67)	863.20 (±447.33)	1	935.46 (±391.33)	669.18 (±250.88)	0.205	0.879
dP/dt max. (mmHg/s)	7738.79 (±885.73)	6650.58 (±1510.60)	0.337	6933.16 (±1810.65)	6231 (±1473.95)	1	1
PRSW	86.26 (±28.95)	87.90 (±27.04)	1	79.32 (±19.44)	77.48 (±21.78)	1	1
ESPVR	14.77 (±8.36)	19.11 (±8.44)	1	15.76 (±11.01)	14.88 (±7.66)	1	1
Diastolic parameters							
Tau (ms)	5.44 (±1.08)	5.42 (±1.24)	1	5.21 (±1.11)	5.66 (±1.80)	1	1
EDPVR	0.27 (±0.25)	0.27 (±0.14)	1	0.19 (±0.09)	0.29 (±0.13)	0.439	1
dP/dt min. (mmHg/s)	-7361.30 (±941.17)	-6643.33 (±1613.47)	1	-6961.90 (±1515.91)	-6545.75 (±1483.59)	1	1

AngII: Angiotensin-II, n = number of mice, Tem.: Temperature, HR: Heart rate, ESP: End-systolic pressure, EDP: End-diastolic pressure, ESV: End-systolic volume, EDV: End-diastolic volume, SV: Stroke volume, CO: Cardiac output, EF: Ejection fraction, dP/dt max.: Maximum pressure increase, PRSW: Preload recruitable stroke work, ESPVR: End-systolic pressure-volume-relation, EDPVR: End-diastolic pressure-volume-relation, dP/dt min.: Minimal pressure increase, p-1: p-value of comparison between WT-NaCl and WT-AngII, p-2: p-value of comparison between Orai1^{CM-KO}-NaCl and Orai1^{CM-KO}-AngII, p-3: p-value of comparison between WT-AngII and KO^{CM}-AngII. Values are given as mean ± SD.

4. Discussion

During heart failure the initially compensatory activation of the renin-angiotensin-aldosterone (RAAS) system turns into a chronic deleterious stimulus for the cardiovascular system; this chronic neurohumoral stimulation includes different important remodeling mechanisms, which are, in part, studied in models of chronic AngII treatment [1,54]. Therefore, we analyzed here the role of Orai1 under AngII stress. Knockdown of Orai1 has been reported to partially reduce the development of neurohumoral-induced cellular hypertrophy in cultured rat neonatal cells [25]. In this study, we aimed to assess whether Orai1 indeed contributes to cardiomyocyte hypertrophy and other features of pathological remodeling *in vivo*. We showed that the genetic deletion of the Orai1 gene is sufficient to completely abolish AngII-induced hypertrophy in mouse embryonic cardiomyocytes. To circumvent potential effects of Orai1 deletion during early development, we generated and studied a cardiomyocyte-specific and temporally inducible Orai1 knockout mouse line. Induction of Orai1 deletion in adult mice did not evoke changes in cardiac contractility or allometric parameters. Counterintuitively, Orai1 deletion in cardiomyocytes aggravated AngII-induced cardiomyocyte hypertrophy and fibrosis.

4.1. *In Vitro* Analysis of Orai1 in Embryonic Cardiomyocytes

We reported here that complete deletion of Orai1 in embryonic mouse cardiomyocytes (E18.5) blunted the AngII-induced hypertrophy. In addition, we showed that at this embryonic stage the cardiomyocytes express Orai1 proteins and we included cells from Orai1-deficient mice in an analysis to investigate the specificity of our anti-Orai1 antibody. Importantly, cells isolated from heterozygous embryos showed detectable Orai1 expression and developed similar cellular hypertrophy in response to AngII, showing that one allele is sufficient to fully mediate Orai1-mediated cellular hypertrophy. Nevertheless, in this cellular model, critical parameters with impact on remodeling in the whole heart *in vivo*-like wall stress, synchronization of electrical activity, the influence of systemic catecholamines, or the contribution of nonmyocytes (e.g., fibroblasts, macrophages, or immune cells) were not taken into account. Therefore, we used a Cre/loxP-mediated approach to delete Orai1 in adult cardiomyocytes since a systemic pharmacological approach that allows selective and efficient inhibition of Orai1 channels in cardiomyocytes is not feasible.

4.2. Impact of Specific Cardiomyocyte Deletion of Orai1 on the Adult Heart

To causally determine the role of Orai1 in the adult heart we inactivated Orai1 expression in adult cardiomyocytes. We included different control groups to determine the effect of tamoxifen or Cre expression (please see short discussion in Supplementary Materials). Based on our experiments with mTmG reporter mice [47], we expected to have an efficient Cre-mediated recombination in adult cardiomyocytes in more than 99% of the cells. We observed by qPCR a reduction in *Orai1* expression by $52 \pm 13\%$ in heart samples and $81.4 \pm 5.4\%$ in cardiomyocytes isolated by Langendorff perfusion from Orai1^{CM-KO} mice. The remaining expression most likely reflected the contribution of nonmyocytes as Orai1 expression in α -Actinin-negative cells isolated from embryonic heart was also found in our study.

The analysis of cardiac contractility under basal conditions by PV loop analysis in Orai1^{CM-KO} mice in comparison to the control group (Orai1^{flox/flox}/ α MHC-Cre^{pos} mice treated with Miglyol) was performed 4 weeks following induction of Orai1 deletion, when transient effects of tamoxifen treatment on cardiac function [55] were not expected. No differences in cardiac function were observed in Orai1^{CM-KO} mice. Specifically, cardiac output, ejection fraction, EDPVR, or preload recruitable stroke work were unaltered. Histological analysis of cardiomyocyte cross-sectional area and collagen deposition (fibrosis) were also unchanged. No signs of heart failure with reduced ejection fraction or of heart failure with preserved ejection fraction (diastolic dysfunction) could be detected in Orai1^{CM-KO} mice. The absence of systolic or diastolic dysfunction in Orai1^{CM-KO} mice was in contrast with the effect

of the deletion of *Stim1*, a critical regulator of *Orai1* activity that leads to reduced cardiac function under basal conditions already 40 days after induction of *Stim1* deletion [56]. These differences in the phenotype between *Orai1*^{CM-KO} mice and *Stim1*^{CM-KO} mice indicate that STIM1 has targets additional to *Orai1* in cardiomyocytes, which might include voltage-gated Ca²⁺ channels [57,58]. Nonetheless, we cannot discard long-term effects of *Orai1* deletion in the adult heart during aging, like those observed in other mouse model with cardiomyocyte-restricted ablation of *Stim1* [59,60].

A possible reason for the absence of obvious changes in cardiac function in *Orai1*^{CM-KO} mice might be that the function of *Orai1* is reduced in naïve adult cardiomyocytes [33]; reduction in expression of *Orai1* in the adulthood was already reported in mice [31]. Another possibility is that the lack of *Orai1* was compensated by the other members of the *Orai* family, such as *Orai2* or *Orai3*. Whereas there are no reports about the functional role of *Orai2* in cardiomyocytes or for cardiac function, *Orai3* regulates a constitutive Ca²⁺ entry in adult left ventricular cardiomyocytes [33,61]. In an in vivo model where *Orai1* (also *Orai3*) expression was reduced by and siRNA-based approach in adult ventricular rat cardiomyocytes, the expression of *Orai3* was increased under basal conditions and after abdominal aortic banding; moreover, the constitutive Ca²⁺ entry in adult left ventricular cardiomyocytes was increased after *Orai1* silencing and abolished when *Orai3* was silenced [61]. Very recently it was briefly reported that cardiomyocyte-specific deletion of *Orai3* causes dilated cardiomyopathy in mice at 4 months of age and the cardiac remodeling was more aggravated in younger mice during aortic banding [62]. In isolated cardiomyocytes from *Orai1*^{CM-KO} mice, we observed unchanged expression of *Orai2* compared to controls and a downregulation of *Orai3* (together with *Stim2* and the SOCE-associated regulatory factor, *Saraf*), pointing out a tight and mutual regulation in expression of these constituents and regulators of SOCE. On the other hand, the amplitude of store-operated Ca²⁺ entry (SOCE), which correlates with the abundance of *Orai1* [25], was significantly lower in adult compared to embryonic cardiomyocytes [23] and, accordingly, the lack of *Orai1* may be dispensable for cardiac function in adult mice. Since SOCE was reactivated following induction of hypertrophy by neurohumoral stimuli, including AngII treatment in adult cardiomyocytes [23], we next challenged *Orai1*^{CM-KO} mice with chronic AngII treatment.

We and others observed changes in the expression of *Orai* subtypes and of other regulators of SOCE when the expression of one of those proteins was altered; in addition, there was a complex mutual regulation by individual *Orai* subtypes as observed in cells from *Orai1*- and *Orai2*-single KO mice and *Orai1/2* double-deficient mice as shown in different T cells subtypes or in mast cells [63,64]. Thus, to obtain a deeper understanding of the contribution of *Orai* proteins in cardiac remodeling, more expansive approaches will be required that include single and compound KO models with cardiomyocyte-specific deletion of genes encoding the corresponding *Orai* subtypes.

4.3. Protective Function of *Orai1* Proteins in Adult Cardiomyocytes During Neurohumorally Induced Cardiac Hypertrophy

In contrast to the expectation from embryonic cardiomyocytes, where hypertrophy was blunted when *Orai1* expression was entirely abrogated by *Orai1* deletion, cardiac hypertrophy indices were not different in adult *Orai1*^{CM-KO} mice compared to control mice, and, remarkably, the interstitial collagen deposition as well as the cardiomyocyte cross-sectional area were significantly increased. From the comparison of absolute values of some functional parameters (i.e., EF) between Figures 2 and 3, some discrepancies might be presumed, but it is important to note that the animals analyzed in these experimental groups differed in the fact that we used *Orai1*^{flox/flox}/ α MHC-Cre^{Pos} (+ Miglyol) as control mice in the first one (Figure 2) and *Orai1*^{flox/flox}/ α MHC-Cre^{Neg} (+ tamoxifen) were used as controls in the latter (Figure 3). The reason for these different approaches was that we were concerned and aimed to check for possible tamoxifen effects in our remodeling model. These differences could indicate, in general, that beyond the effect of AngII there could be also an effect of Cre (independent of tamoxifen) and point to the importance of different types of controls during this kind of experiment.

We observed a significant reduction in the ejection fraction in Orai1^{CM-KO} mice at the end of the two weeks of chronic AngII infusion. Accordingly, stroke volumes were also decreased in Orai1^{CM-KO}. These results suggest a rather protective function of Orai1 in adult cardiomyocytes for the maintenance of proper cardiac function under stress conditions. Recently, Horton et al. reported that targeting of one Orai1 allele by a gene-trap approach, which goes along with partial reduction of Orai1 expression in the heart, led to escalation of heart failure development and an increase in mortality evoked by chronic pressure overload [39]. In this study the influence of Orai1 in cardiac non-myocytes or extracardial cells may also contribute to the observed phenotype and it remains to be analyzed in mouse lines in which Orai1 deleted other cell types relevant for cardiac remodeling, like cardiac fibroblasts or macrophages. Additionally, there were discrepancies between the gene-trapping approaches that most likely generated a hypomorphic Orai1 allele [65] compared to the mouse model generated by defined deletion of exons 2 and 3 by homologous recombination [37]. Very recently it was shown that Orai1 inhibition in adult murine cardiomyocytes by the expression of a dominant-negative mutant (Orai1^{R91W}) or by pharmacological treatment ameliorated the reduction in systolic function provoked by pressure overload [66]. This approach differed from ours as expression of a dominant negative Orai1 subtype may affect all channel entities consisting of Orai1 proteins, and the composition of the channel complex triggered by AngII in cardiomyocytes is still unknown. In addition, the phenotype obtained by systemic pharmacological inhibition of Orai1-containing channel complexes can also be mediated by cardiac nonmyocytes and extracardial actions of this substance. Moreover, the signaling pathways contributing to AngII-induced remodeling as analyzed in our study may differ compared to the pressure overload-evoked remodeling process as seen in AngII Type 1A receptor KO mice, which are protected from AngII-induced hypertrophy but not from pressure overload hypertrophy [67]. Despite the finding from this former study that Orai1 is a critical mediator for Ca²⁺ entry and cardiac remodeling, the composition of the channel complex triggered by AngII in cardiomyocytes is still unknown. Nevertheless, both the study by Bartoli et al. and ours are in agreement with the concept of Orai1 as a critical constituent of the Ca²⁺ entry pathway mediating cardiomyocyte and cardiac remodeling with Orai1 acting in concert with other channel proteins that can take over and even overcompensate when Orai1 is absent. Based on our results obtained by selective deletion of Orai1, it is well conceivable that other constituents of the channel complex, such as Orai2 and/or Orai3, might take over. Orai1 is known to interact with Orai2 or Orai3 in several cell systems functionally as well as physically, and such behavior has been reported by others and by us in lymphocytes and mast cells, respectively [63,64].

4.4. Cardiac Transcriptional Changes in the Absence of Orai1 in Cardiomyocytes after AngII-Evoked Cardiac Remodelling

Transcriptional upregulation of Orai1-3 and reactivation of SOCE amplitude under stress condition was reported previously, including upregulation of SOCE activity after TAC [23] and upregulation of Orai1 mRNA and protein expression after TAC and myocardial infarction [31]. These results imply that Orai-mediated signaling is part of the compensatory signaling cascade that includes control of transcriptional programs and complex Ca²⁺ homeostatic regulatory mechanisms during the development of pathological cardiac hypertrophy in adulthood [68]. We observed that the upregulation of *Orai3* and *Stim1* expression evoked by neurohumoral stress via chronic AngII treatment depends completely on the expression of Orai1. Previous work in immune cells [69] but also in neonatal cardiomyocytes [31] established that the signaling cascade downstream of Orai1 is associated with the activation of the protein phosphatase calcineurin. Calcineurin is a key player in the development of cardiac hypertrophy [70] and it is able to activate two important transcriptional regulatory pathways, one through the nuclear factor of activated T cells (NFAT) and the other through the myocyte enhancer factor 2 (MEF2) [71,72].

Orai1-deletion in cardiomyocytes does not seem to affect MEF2a signaling as expression of *Mef2a* itself and its target *Myomaxin* was similarly regulated in control and Orai1^{CM-KO}. An increase in AngII-evoked upregulation of *Myomaxin* was found to depend on TRPC1/TRPC4 that mediates a Ca²⁺

entry in cardiomyocytes described as BGCE (background Ca^{2+} entry pathway). TRPC1/TRPC4 deletion together with reduced BGCE preclude AngII-evoked rise in electrically triggered Ca^{2+} transients and decreases AngII-induced hypertrophy and fibrosis in vivo [9].

On the other hand, our expression analysis in hearts of *Orai1*^{CM-KO} mice suggests that *Orai1* may contribute to the calcineurin-NFAT signaling axis as AngII-evoked RCAN1 upregulation is reduced in *Orai1*^{CM-KO} hearts. The current study showed a reduced expression of *Rcan1* and enhanced cardiac remodeling in the absence of *Orai1*, whereas reduced *Rcan1* expression in the absence of TRPC1/TRPC4 led to a decrease in the development of cardiac hypertrophy [9]. Based on these observations, it is tempting to speculate how two distinct Ca^{2+} entry pathways in cardiomyocytes could regulate the development of the cardiac remodeling differentially. The results contribute to understand the proposed involvement of transcriptional pathways regulated by the calcineurin-NFAT and/or the CaMKII (Ca^{2+} /calmodulin-dependent protein kinase II)-MEF2 axis. This is not surprising since RCAN1 has been described to play a dual role during the development of cardiac hypertrophy as it can either facilitate or suppress cardiac calcineurin signaling [73].

Additional and yet to be discovered are properties of *Orai1* and TRPC1/TRPC4 proteins that are not directly related to their Ca^{2+} -conducting function. It is still not clear to which extent the solely Ca^{2+} -conducted-by-cation channel is responsible for the transcriptional regulation and functional/morphological changes observed during cardiac remodeling. It is plausible that downstream signaling, including transcriptional changes, is regulated independently of the channel function, as identified in other Ca^{2+} channels [74,75]. Nevertheless, the upregulation of the negative regulator of calcineurin, *Myoz2* (*Calsarcin-1*) was abrogated in the absence of *Orai1* in AngII-treated hearts. This might give an additional hint how cardiomyocyte hypertrophy and fibrosis may come about in *Orai1*^{CM-KO} mice after AngII infusion as *calsarcin-1*-deficient mice exhibit stress-evoked cardiomyocyte hypertrophy as a consequence of inappropriate calcineurin activation [76,77].

Together, our results reveal a critical role of *Orai1* for fine-tuning cardiac remodeling. They indicate an inverse mode of action between early developmental stages and disease progression in the adulthood, as it operates as a crucial mediator for the hypertrophic response in embryonic myocytes but as a limiting determinant in hypertrophy and fibrosis in neurohumorally evoked cardiac pathology in adults.

Supplementary Materials: The following are available online at <http://www.mdpi.com/2073-4409/9/5/1092/s1>. Figure S1: Induction of cellular hypertrophy in neonatal cardiomyocytes from wild-type mice. Figure S2: Efficiency and specificity of Cre-expression under the αMHC promoter. Table S1: Allometric analysis of *Orai1*^{fx/fx} $\alpha\text{MHC}/\text{Cre}^{\text{pos}}$ mice. Table S2: Allometric analysis of *Orai1*-WT and *Orai1*^{CM-KO} mice after angiotensin-II treatment. Table S3: Primers used for qPCR analysis. Supplementary Discussion. Gene deletion of *Orai1* and controls for tamoxifen treatment or Cre expression.

Author Contributions: Conceptualization, S.S., M.F., and J.E.C.L.; Data curation, S.S., M.B., R.M., C.R., and J.E.C.L.; Formal analysis, S.S. and J.E.C.L.; Funding acquisition, M.F. and J.E.C.L.; Investigation, S.S., M.F., and J.E.C.L.; Methodology, S.S. and J.E.C.L.; Project administration, M.F. and J.E.C.L.; Resources, V.F., P.W., M.F., and J.E.C.L.; Supervision, M.F. and J.E.C.L.; Visualization, S.S. and J.E.C.L.; Writing—original draft, S.S., M.F., and J.E.C.L.; Writing—review & editing, all authors. All authors have read and agreed to the published version of the manuscript.

Funding: This work was supported by the DZHK (German Centre for Cardiovascular Research), the BMBF (German Ministry of Education and Research), the Deutsche Forschungsgemeinschaft (DFG, German Research Foundation): Project-ID 239283807—Transregional Collaborative Research Centre-152 (TRR 152)-, FOR 2289, the Collaborative Research Center (SFB) 1118, GRK1326, the DIAMICOM graduate school (GRK 1874), a Baden-Württemberg federal state Innovation funds, and the DFG FL 153/10-2 (VF).

Acknowledgments: We are thankful to Stefan Offermanns (Max Planck Institute for Heart and Lung Research, Germany) who kindly provided the $\alpha\text{MHC}/\text{CreERT2}$ mice, and to Manuela Ritzal, Hans-Peter Gensheimer, Ralph Röth, and the team from the Interfakultäre Biomedizinische Forschungseinrichtung (IBF) from the Heidelberg University for expert technical assistance.

Conflicts of Interest: The authors declare no conflict of interest.

References

1. Hartupee, J.; Mann, D.L. Neurohormonal activation in heart failure with reduced ejection fraction. *Nat. Rev. Cardiol.* **2016**, *14*, 30–38. [[CrossRef](#)] [[PubMed](#)]
2. Wettschureck, N.; Offermanns, S. Mammalian G Proteins and Their Cell Type Specific Functions. *Physiol. Rev.* **2005**, *85*, 1159–1204. [[CrossRef](#)] [[PubMed](#)]
3. Goonasekera, S.A.; Molkentin, J.D. Unraveling the secrets of a double life: Contractile versus signaling Ca²⁺ in a cardiac myocyte. *J. Mol. Cell. Cardiol.* **2012**, *52*, 317–322. [[CrossRef](#)] [[PubMed](#)]
4. Luo, M.; Anderson, M.E. Mechanisms of altered Ca²⁺ handling in heart failure. *Circ. Res.* **2013**, *113*, 690–708. [[CrossRef](#)] [[PubMed](#)]
5. Eder, P. Cardiac Remodeling and Disease: SOCE and TRPC Signaling in Cardiac Pathology. *Advances in Experimental Medicine and Biology* **2017**, *993*, 505–521. [[CrossRef](#)]
6. Freichel, M.; Berlin, M.; Schürger, A.; Mathar, I.; Bacmeister, L.; Medert, R.; Frede, W.; Marx, A.; Segin, S.; Londoño, J.E.C.; et al. TRP Channels in the Heart. In *Methods for Neural Ensemble Recordings*; Informa UK Limited: Colchester, UK, 2017; pp. 149–185.
7. Numaga-Tomita, T.; Oda, S.; Shimauchi, T.; Nishimura, A.; Mangmool, S.; Nishida, M. TRPC3 Channels in Cardiac Fibrosis. *Front. Cardiovasc. Med.* **2017**, *4*, 56. [[CrossRef](#)]
8. Yamaguchi, Y.; Iribe, G.; Nishida, M.; Naruse, K. Role of TRPC3 and TRPC6 channels in the myocardial response to stretch: Linking physiology and pathophysiology. *Prog. Biophys. Mol. Boil.* **2017**, *130*, 264–272. [[CrossRef](#)]
9. Londoño, J.E.C.; Tian, Q.; Hammer, K.; Schröder, L.; Londoño, J.C.; Reil, J.C.; He, T.; Oberhofer, M.; Mannebach, S.; Mathar, I.; et al. A background Ca²⁺ entry pathway mediated by TRPC1/TRPC4 is critical for development of pathological cardiac remodelling. *Eur. Hear. J.* **2015**, *36*, 2257–2266. [[CrossRef](#)]
10. Parekh, A.B.; Penner, R. Store depletion and calcium influx. *Physiol. Rev.* **1997**, *77*, 901–930. [[CrossRef](#)]
11. Parekh, A.B.; Putney, J. Store-Operated Calcium Channels. *Physiol. Rev.* **2005**, *85*, 757–810. [[CrossRef](#)]
12. Feske, S.; Gwack, Y.; Prakriya, M.; Srikanth, S.; Puppel, S.-H.; Tanasa, B.; Hogan, P.G.; Lewis, R.S.; Daly, M.; Rao, A. A mutation in Orai1 causes immune deficiency by abrogating CRAC channel function. *Nature* **2006**, *441*, 179–185. [[CrossRef](#)] [[PubMed](#)]
13. Prakriya, M.; Feske, S.; Gwack, Y.; Srikanth, S.; Rao, A.; Hogan, P.G. Orai1 is an essential pore subunit of the CRAC channel. *Nature* **2006**, *443*, 230–233. [[CrossRef](#)] [[PubMed](#)]
14. Vig, M.; Peinelt, C.; Beck, A.; Koomoa, D.L.; Rabah, D.; Koblan-Huberson, M.; Kraft, S.; Turner, H.; Fleig, A.; Penner, R.; et al. CRACM1 Is a Plasma Membrane Protein Essential for Store-Operated Ca²⁺ Entry. *Science* **2006**, *312*, 1220–1223. [[CrossRef](#)] [[PubMed](#)]
15. Zhang, S.L.; Yeromin, A.V.; Zhang, X.H.-F.; Yu, Y.; Safrina, O.; Penna, A.; Roos, J.; Stauderman, K.A.; Cahalan, M.D. Genome-wide RNAi screen of Ca²⁺ influx identifies genes that regulate Ca²⁺ release-activated Ca²⁺ channel activity. *Proc. Natl. Acad. Sci. USA* **2006**, *103*, 9357–9362. [[CrossRef](#)] [[PubMed](#)]
16. Hou, X.; Pedi, L.; Diver, M.M.; Long, S.B. Crystal structure of the calcium release-activated calcium channel Orai. *Science* **2012**, *338*, 1308–1313. [[CrossRef](#)]
17. Gross, S.A.; Wissenbach, U.; Philipp, S.E.; Freichel, M.; Cavalié, A.; Flockerzi, V.; Guy, J.E.; Whittle, E.; Kumaran, D.; Lindqvist, Y.; et al. Murine ORAI2 Splice Variants Form Functional Ca²⁺-Release-activated Ca²⁺(CRAC) Channels. *J. Biol. Chem.* **2007**, *282*, 19375–19384. [[CrossRef](#)] [[PubMed](#)]
18. Feske, S. CRAC channels and disease – From human CRAC channelopathies and animal models to novel drugs. *Cell Calcium* **2019**, *80*, 112–116. [[CrossRef](#)]
19. Zhang, S.L.; Yu, Y.; Roos, J.; Kozak, J.A.; Deerinck, T.J.; Ellisman, M.H.; Stauderman, K.A.; Cahalan, M.D. STIM1 is a Ca²⁺ sensor that activates CRAC channels and migrates from the Ca²⁺ store to the plasma membrane. *Nature* **2005**, *437*, 902–905. [[CrossRef](#)]
20. Stathopoulos, P.B.; Li, G.-Y.; Plevin, M.; Ames, J.B.; Ikura, M. Stored Ca²⁺ Depletion-induced Oligomerization of Stromal Interaction Molecule 1 (STIM1) via the EF-SAM Region: An Initiation Mechanism for Capacitive Ca²⁺ Entry. *J. Biol. Chem.* **2006**, *281*, 35855–35862. [[CrossRef](#)]
21. Liou, J.; Kim, M.L.; Heo, W.D.; Jones, J.T.; Myers, J.W.; Ferrell, J.E.; Meyer, T. STIM Is a Ca²⁺ Sensor Essential for Ca²⁺-Store-Depletion-Triggered Ca²⁺ Influx. *Curr. Biol.* **2005**, *15*, 1235–1241. [[CrossRef](#)]

22. Roos, J.; Digregorio, P.J.; Yeromin, A.V.; Ohlsen, K.; Lioudyno, M.; Zhang, S.; Safrina, O.; Kozak, J.A.; Wagner, S.L.; Cahalan, M.D.; et al. STIM1, an essential and conserved component of store-operated Ca²⁺ channel function. *J. Cell Biol.* **2005**, *169*, 435–445. [[CrossRef](#)] [[PubMed](#)]
23. Luo, X.; Hojdayev, B.; Jiang, N.; Wang, Z.V.; Tandan, S.; Rakalin, A.; Rothermel, B.A.; Gillette, T.G.; Hill, J. STIM1-dependent store-operated Ca²⁺ entry is required for pathological cardiac hypertrophy. *J. Mol. Cell. Cardiol.* **2011**, *52*, 136–147. [[CrossRef](#)] [[PubMed](#)]
24. Hulot, J.-S.; Fauconnier, J.; Ramanujam, D.; Chaanine, A.; Aubart, F.; Sassi, Y.; Merkle, S.; Cazorla, O.; Ouillé, A.; Dupuis, M.; et al. Critical role for stromal interaction molecule 1 in cardiac hypertrophy. *Circulation* **2011**, *124*, 796–805. [[CrossRef](#)] [[PubMed](#)]
25. Völkers, M.; Salz, M.; Herzog, N.; Frank, D.; Dolatabadi, N.; Frey, N.; Gude, N.; Friedrich, O.; Koch, W.J.; Katus, H.A.; et al. Orai1 and Stim1 regulate normal and hypertrophic growth in cardiomyocytes. *J. Mol. Cell. Cardiol.* **2010**, *48*, 1329–1334. [[CrossRef](#)]
26. Hunton, D.L.; Zou, L.; Pang, Y.; Marchase, R.B. Adult rat cardiomyocytes exhibit capacitative calcium entry. *Am. J. Physiol. Circ. Physiol.* **2004**, *286*, H1124–H1132. [[CrossRef](#)]
27. Touchberry, C.; Elmore, C.J.; Nguyen, T.M.; Andresen, J.J.; Zhao, X.; Orange, M.; Weisleder, N.; Brotto, M.; Claycomb, W.C.; Wacker, M.J. Store-operated calcium entry is present in HL-1 cardiomyocytes and contributes to resting calcium. *Biochem. Biophys. Res. Commun.* **2011**, *416*, 45–50. [[CrossRef](#)]
28. Hunton, D.L.; A Lucchesi, P.; Pang, Y.; Cheng, X.; Dell'Italia, L.J.; Marchase, R.B. Capacitative Calcium Entry Contributes to Nuclear Factor of Activated T-cells Nuclear Translocation and Hypertrophy in Cardiomyocytes. *J. Biol. Chem.* **2002**, *277*, 14266–14273. [[CrossRef](#)]
29. Nakayama, H.; Wilkin, B.J.; Bodi, I.; Molkentin, J.D. Calcineurin-dependent cardiomyopathy is activated by TRPC in the adult mouse heart. *FASEB J.* **2006**, *20*, 1660–1670. [[CrossRef](#)]
30. Ju, Y.-K.; Chu, Y.; Chaudhry, H.; Lai, D.; Gervasio, O.L.; Graham, R.M.; Cannell, M.B.; Allen, D.G. Store-Operated Ca²⁺Influx and Expression of TRPC Genes in Mouse Sinoatrial Node. *Circ. Res.* **2007**, *100*, 1605–1614. [[CrossRef](#)]
31. Völkers, M.; Dolatabadi, N.; Gude, N.; Most, P.; Sussman, M.A.; Hassel, D. Orai1 deficiency leads to heart failure and skeletal myopathy in zebrafish. *J. Cell Sci.* **2012**, *125*, 287–294. [[CrossRef](#)]
32. Dai, F.; Zhang, Y.; Wang, Q.; Li, D.; Yang, Y.; Ma, S.; Yang, D. Overexpression of SARAF Ameliorates Pressure Overload-Induced Cardiac Hypertrophy Through Suppressing STIM1-Orai1 in Mice. *Cell. Physiol. Biochem.* **2018**, *47*, 817–826. [[CrossRef](#)] [[PubMed](#)]
33. Benard, L.; Lompré, A.-M. STIM1 and Orai in cardiac hypertrophy and vascular proliferative diseases. *Front. Biosci.* **2013**, *5*, 766–773. [[CrossRef](#)]
34. Collins, H.E.; Zhu-Mauldin, X.; Marchase, R.B.; Chatham, J.C. STIM1/Orai1-mediated SOCE: current perspectives and potential roles in cardiac function and pathology. *Am. J. Physiol. Circ. Physiol.* **2013**, *305*, H446–H458. [[CrossRef](#)] [[PubMed](#)]
35. Avila-Medina, J.; Mayoral-Gonzalez, I.; Domínguez-Rodríguez, A.; Gallardo-Castillo, I.; Ribas, J.; Ordóñez, A.; Rosado, J.A.; Smani, T. The Complex Role of Store Operated Calcium Entry Pathways and Related Proteins in the Function of Cardiac, Skeletal and Vascular Smooth Muscle Cells. *Front. Physiol.* **2018**, *9*, 9. [[CrossRef](#)] [[PubMed](#)]
36. Rosenberg, P.; Katz, D.; Bryson, V. SOCE and STIM1 signaling in the heart: Timing and location matter. *Cell Calcium* **2019**, *77*, 20–28. [[CrossRef](#)] [[PubMed](#)]
37. Gwack, Y.; Srikanth, S.; Oh-Hora, M.; Hogan, P.G.; Lamperti, E.D.; Yamashita, M.; Gelinas, C.; Neems, D.S.; Sasaki, Y.; Feske, S.; et al. Hair Loss and Defective T- and B-Cell Function in Mice Lacking ORAI1. *Mol. Cell. Biol.* **2008**, *28*, 5209–5222. [[CrossRef](#)] [[PubMed](#)]
38. Petersen, C.E.; Wolf, M.J.; Smyth, J.T. Suppression of store-operated calcium entry causes dilated cardiomyopathy of the Drosophila heart. *Biol. Open* **2020**, *9*, bio049999. [[CrossRef](#)]
39. Horton, J.S.; Buckley, C.L.; Alvarez, E.M.; Schorlemmer, A.; Stokes, A. The calcium release-activated calcium channel Orai1 represents a crucial component in hypertrophic compensation and the development of dilated cardiomyopathy. *Channels* **2013**, *8*, 35–43. [[CrossRef](#)]
40. Sabourin, J.; Bartoli, F.; Antigny, F.; Gomez, A.-M.; Benitah, J.-P. Transient Receptor Potential Canonical (TRPC)/Orai1-dependent Store-operated Ca²⁺Channels. *J. Biol. Chem.* **2016**, *291*, 13394–13409. [[CrossRef](#)]

41. Wang, Y.; Li, Z.C.; Zhang, P.; Poon, E.; Kong, C.W.; Boheler, K.R.; Huang, Y.; Li, R.A.; Yao, X. Nitric Oxide-cGMP-PKG Pathway Acts on Orai1 to Inhibit the Hypertrophy of Human Embryonic Stem Cell-Derived Cardiomyocytes. *Stem Cells* **2015**, *33*, 2973–2984. [[CrossRef](#)]
42. Zheng, C.; Lo, C.-Y.; Meng, Z.; Li, Z.; Zhong, M.; Zhang, P.; Lu, J.; Yang, Z.; Yan, F.; Zhang, Y.; et al. Gastrodin Inhibits Store-Operated Ca²⁺ Entry and Alleviates Cardiac Hypertrophy. *Front. Pharmacol.* **2017**, *8*, 534. [[CrossRef](#)]
43. McCarl, C.-A.; Picard, C.; Khalil, S.; Kawasaki, T.; Röther, J.; Papolos, A.; Kutok, J.; Hivroz, C.; LeDeist, F.; Plogmann, K.; et al. ORAI1 deficiency and lack of store-operated Ca²⁺ entry cause immunodeficiency, myopathy, and ectodermal dysplasia. *J. Allergy Clin. Immunol.* **2009**, *124*, 1311–1318.e7. [[CrossRef](#)]
44. Ahuja, M.; Schwartz, D.M.; Tandon, M.; Son, A.; Zeng, M.; Swaim, W.; Eckhaus, M.; Hoffman, V.; Cui, Y.; Xiao, B.; et al. Orai1-Mediated Antimicrobial Secretion from Pancreatic Acini Shapes the Gut Microbiome and Regulates Gut Innate Immunity. *Cell Metab.* **2017**, *25*, 635–646. [[CrossRef](#)]
45. Schwenk, F.; Baron, U.; Rajewsky, K. A cre -transgenic mouse strain for the ubiquitous deletion of loxP -flanked gene segments including deletion in germ cells. *Nucleic Acids Res.* **1995**, *23*, 5080–5081. [[CrossRef](#)] [[PubMed](#)]
46. Takefuji, M.; Wirth, A.; Lukasova, M.; Takefuji, S.; Boettger, T.; Braun, T.; Althoff, T.; Offermanns, S.; Wettschureck, N. G13-Mediated Signaling Pathway Is Required for Pressure Overload-Induced Cardiac Remodeling and Heart Failure. *Circulation* **2012**, *126*, 1972–1982. [[CrossRef](#)] [[PubMed](#)]
47. Muzumdar, M.; Tasic, B.; Miyamichi, K.; Li, L.; Luo, L. A global double-fluorescent Cre reporter mouse. *Genes* **2007**, *45*, 593–605. [[CrossRef](#)] [[PubMed](#)]
48. Pacher, P.; Nagayama, T.; Mukhopadhyay, P.; Bátkai, S.; Kass, D.A. Measurement of cardiac function using pressure–volume conductance catheter technique in mice and rats. *Nat. Protoc.* **2008**, *3*, 1422–1434. [[CrossRef](#)]
49. Bacmeister, L.; Segin, S.; Medert, R.; Lindner, D.; Freichel, M.; Londoño, J.E.C. Assessment of PEEP-Ventilation and the Time Point of Parallel-Conductance Determination for Pressure-Volume Analysis Under β -Adrenergic Stimulation in Mice. *Front. Cardiovasc. Med.* **2019**, *6*, 36. [[CrossRef](#)]
50. Wissenbach, U.; Philipp, S.E.; Gross, S.A.; Cavalié, A.; Flockerzi, V. Primary structure, chromosomal localization and expression in immune cells of the murine ORAI and STIM genes. *Cell Calcium* **2007**, *42*, 439–446. [[CrossRef](#)]
51. Sachdeva, R.; Fleming, T.; Schumacher, D.; Homberg, S.; Stolz, K.; Mohr, F.; Wagner, A.H.; Tsvilovskyy, V.; Mathar, I.; Freichel, M. Methylglyoxal evokes acute Ca²⁺ transients in distinct cell types and increases agonist-evoked Ca²⁺ entry in endothelial cells via CRAC channels. *Cell Calcium* **2019**, *78*, 66–75. [[CrossRef](#)] [[PubMed](#)]
52. Varga-Szabo, D.; Braun, A.; Nieswandt, B. STIM and Orai in platelet function. *Cell Calcium* **2011**, *50*, 270–278. [[CrossRef](#)] [[PubMed](#)]
53. Cheng, K.T.; Liu, X.; Ong, H.L.; Swaim, W.; Ambudkar, I.S. Local Ca²⁺ entry via Orai1 regulates plasma membrane recruitment of TRPC1 and controls cytosolic Ca²⁺ signals required for specific cell functions. *PLoS Biol.* **2011**, *9*, e1001025. [[CrossRef](#)]
54. Kim, H.J.; Lv, P.; Sihm, C.-R.; Yamoah, E.N. Cellular and Molecular Mechanisms of Autosomal Dominant Form of Progressive Hearing Loss, DFNA2*. *J. Biol. Chem.* **2010**, *286*, 1517–1527. [[CrossRef](#)] [[PubMed](#)]
55. Koitabashi, N.; Bedja, D.; Zaiman, A.L.; Pinto, Y.M.; Zhang, M.; Gabrielson, K.L.; Takimoto, E.; Kass, D.A. Avoidance of transient cardiomyopathy in cardiomyocyte-targeted tamoxifen-induced MerCreMer gene deletion models. *Circ. Res.* **2009**, *105*, 12–15. [[CrossRef](#)]
56. Parks, C.; Alam, M.A.; Sullivan, R.; Mancarella, S. STIM1-dependent Ca²⁺ microdomains are required for myofilament remodeling and signaling in the heart. *Sci. Rep.* **2016**, *6*, 25372. [[CrossRef](#)] [[PubMed](#)]
57. Park, C.Y.; Shcheglovitov, A.; Dolmetsch, R. The CRAC Channel Activator STIM1 Binds and Inhibits L-Type Voltage-Gated Calcium Channels. *Science* **2010**, *330*, 101–105. [[CrossRef](#)] [[PubMed](#)]
58. Wang, Y.; Deng, X.; Mancarella, S.; Hendron, E.; Eguchi, S.; Soboloff, J.; Tang, X.D.; Gill, D.L. The Calcium Store Sensor, STIM1, Reciprocally Controls Orai and CaV1.2 Channels. *Science* **2010**, *330*, 105–109. [[CrossRef](#)]
59. Collins, H.E.; He, L.; Zou, L.; Qu, J.; Zhou, L.; Litovsky, S.H.; Yang, Q.; Young, M.E.; Marchase, R.B.; Chatham, J.C. Stromal interaction molecule 1 is essential for normal cardiac homeostasis through modulation of ER and mitochondrial function. *Am. J. Physiol. Circ. Physiol.* **2014**, *306*, H1231–H1239. [[CrossRef](#)]

60. Collins, H.E.; Pat, B.M.; Zou, L.; Litovsky, S.H.; Wende, A.R.; Young, M.E.; Chatham, J.C. Novel role of the ER/SR Ca²⁺ sensor STIM1 in the regulation of cardiac metabolism. *Am. J. Physiol. Circ. Physiol.* **2019**, *316*, H1014–H1026. [[CrossRef](#)]
61. Saliba, Y.; Keck, M.; Marchand, A.; Atassi, F.; Ouillé, A.; Cazorla, O.; Trebak, M.; Pavoine, C.; Lacampagne, A.; Hulot, J.-S.; et al. Emergence of Orai3 activity during cardiac hypertrophy. *Cardiovasc. Res.* **2014**, *105*, 248–259. [[CrossRef](#)]
62. Mancarella, S.; Kamatham, S. Abstract 922: Cardiac-specific Deletion of Orai3 Channel Causes Dilated Cardiomyopathy. *Circ. Res.* **2019**, *125*, 125. [[CrossRef](#)]
63. Tsvilovskyy, V.; Solís-López, A.; Schumacher, D.; Medert, R.; Roers, A.; Kriebs, U.; Freichel, M. Deletion of Orai2 augments endogenous CRAC currents and degranulation in mast cells leading to enhanced anaphylaxis. *Cell Calcium* **2018**, *71*, 24–33. [[CrossRef](#)]
64. Vaeth, M.; Yang, J.; Yamashita, M.; Zee, I.; Eckstein, M.; Knosp, C.; Kaufmann, U.; Jani, P.K.; Lacruz, R.S.; Flockerzi, V.; et al. ORAI2 modulates store-operated calcium entry and T cell-mediated immunity. *Nat. Commun.* **2017**, *8*, 14714. [[CrossRef](#)] [[PubMed](#)]
65. Vig, M.; DeHaven, W.I.; Bird, G.S.; Billingsley, J.M.; Wang, H.; E Rao, P.; Hutchings, A.B.; Jouvin, M.-H.; Putney, J.; Kinet, J.-P. Defective mast cell effector functions in mice lacking the CRACM1 pore subunit of store-operated calcium release-activated calcium channels. *Nat. Immunol.* **2007**, *9*, 89–96. [[CrossRef](#)] [[PubMed](#)]
66. Bartoli, F.; Bailey, M.A.; Rode, B.; Mateo, P.; Antigny, F.; Bedouet, K.; Gerbaud, P.; Gosain, R.; Plante, J.; Norman, K.; et al. Orai1 Channel Inhibition Preserves Left Ventricular Systolic Function and Normal Ca²⁺ Handling After Pressure Overload. *Circ.* **2020**, *141*, 199–216. [[CrossRef](#)] [[PubMed](#)]
67. Harada, K.; Komuro, I.; Shiojima, I.; Hayashi, D.; Kudoh, S.; Mizuno, T.; Kijima, K.; Matsubara, H.; Sugaya, T.; Murakami, K.; et al. Pressure overload induces cardiac hypertrophy in angiotensin II type 1A receptor knockout mice. *Circulation* **1998**, *97*, 1952–1959. [[CrossRef](#)] [[PubMed](#)]
68. Dewenter, M.; Von Der Lieth, A.; Katus, H.A.; Backs, J. Calcium Signaling and Transcriptional Regulation in Cardiomyocytes. *Circ. Res.* **2017**, *121*, 1000–1020. [[CrossRef](#)]
69. Feske, S.; Skolnik, E.Y.; Prakriya, M. Ion channels and transporters in lymphocyte function and immunity. *Nat. Rev. Immunol.* **2012**, *12*, 532–547. [[CrossRef](#)]
70. Molkentin, J.D.; Lu, J.; Antos, C.L.; Markham, B.; Richardson, J.; Robbins, J.; Grant, S.R.; Olson, E.N. A Calcineurin-Dependent Transcriptional Pathway for Cardiac Hypertrophy. *Cell* **1998**, *93*, 215–228. [[CrossRef](#)]
71. Huang, H.-T.; Brand, O.M.; Mathew, M.; Ignatiou, C.; Ewen, E.P.; McCalmon, S.A.; Naya, F.J. Myomaxin Is a Novel Transcriptional Target of MEF2A That Encodes a Xin-related α -Actinin-interacting Protein. *J. Biol. Chem.* **2006**, *281*, 39370–39379. [[CrossRef](#)]
72. Yang, J.; Rothermel, B.; Vega, R.B.; Frey, N.; McKinsey, T.A.; Olson, E.N.; Bassel-Duby, R.; Williams, R.S. Independent signals control expression of the calcineurin inhibitory proteins MCIP1 and MCIP2 in striated muscles. *Circ. Res.* **2000**, *87*, 61–68. [[CrossRef](#)] [[PubMed](#)]
73. Vega, R.B.; Rothermel, B.A.; Weinheimer, C.J.; Kovacs, A.; Naseem, R.H.; Bassel-Duby, R.; Williams, R.S.; Olson, E.N. Dual roles of modulatory calcineurin-interacting protein 1 in cardiac hypertrophy. *Proc. Natl. Acad. Sci. USA* **2003**, *100*, 669–674. [[CrossRef](#)] [[PubMed](#)]
74. Li, B.; Tadross, M.R.; Tsien, R.W. Sequential ionic and conformational signaling by calcium channels drives neuronal gene expression. *Science* **2016**, *351*, 863–867. [[CrossRef](#)] [[PubMed](#)]
75. Farmer, L.K.; Rollason, R.; Whitcomb, D.J.; Ni, L.; Goodliff, A.; Lay, A.; Birnbaumer, L.; Heesom, K.J.; Xu, S.-Z.; Saleem, M.A.; et al. TRPC6 Binds to and Activates Calpain, Independent of Its Channel Activity, and Regulates Podocyte Cytoskeleton, Cell Adhesion, and Motility. *J. Am. Soc. Nephrol.* **2019**, *30*, 1910–1924. [[CrossRef](#)]

76. Frey, N.; Barrientos, T.; Shelton, J.M.; Frank, D.; Rütten, H.; Gehring, D.; Kuhn, C.; Lutz, M.; Rothermel, B.; Bassel-Duby, R.; et al. Mice lacking calstabin-1 are sensitized to calcineurin signaling and show accelerated cardiomyopathy in response to pathological biomechanical stress. *Nat. Med.* **2004**, *10*, 1336–1343. [[CrossRef](#)]
77. Frank, D.; Kuhn, C.; Van Eickels, M.; Gehring, D.; Hanselmann, C.; Lippl, S.; Will, R.; Katus, H.A.; Frey, N. Calstabin-1 Protects Against Angiotensin-II-Induced Cardiac Hypertrophy. *Circulation* **2007**, *116*, 2587–2596. [[CrossRef](#)]



© 2020 by the authors. Licensee MDPI, Basel, Switzerland. This article is an open access article distributed under the terms and conditions of the Creative Commons Attribution (CC BY) license (<http://creativecommons.org/licenses/by/4.0/>).